

# KINETIC AND ENERGETIC PERFORMANCES OF THERMOMETRIC MATERIAL $\text{TiCo}_{1-x}\text{Mn}_x\text{Sb}$ : MODELLING AND EXPERIMENT

*Volodymyr Krayovskyy, Dr. Sc., Prof., Volodymyr Pashkevych, Ph. Dr., As.-Prof.,  
Mariya Rokomanyuk, PhD-student, Petro Haranuk, Ph. Dr., As.-Prof.,  
Volodymyr Romaka, Dr. Sc., Prof.,  
Lviv Polytechnic National University, Ukraine  
Yuriy Stadnyk, Ph. Dr., Senior Scientist, Lyubov Romaka, Ph. Dr., Senior Scientist,  
Andriy Horyn, Ph. Dr., Senior Research,  
Ivan Franko National University of Lviv, Ukraine  
e-mail: mariya.rokomanyuk@gmail.com*

**Abstract.** The results of a complex study of the semiconductor thermometric material  $\text{TiCo}_{1-x}\text{Mn}_x\text{Sb}$ ,  $x=0.01-0.10$ , for the production of sensitive elements of thermoelectric and electro resistive sensors are presented. Microprobe analysis of the concentration of atoms on the surface of  $\text{TiCo}_{1-x}\text{Mn}_x\text{Sb}$  samples established their correspondence to the initial compositions of the charge, and X-ray phase analysis showed the absence of traces of extraneous phases on their diffractograms. The produced structural studies of the thermometric material  $\text{TiCo}_{1-x}\text{Mn}_x\text{Sb}$  allow to speak about the ordering of its crystal structure, and the substitution of Co atoms on Mn at the 4c position generate structural defects of acceptor nature. The obtained results testify to the homogeneity of the samples and their suitability for the study of electrokinetic performances and the manufacture of sensitive elements of thermocouples.

Modeling of structural, electrokinetic, and energetic performances of  $\text{TiCo}_{1-x}\text{Mn}_x\text{Sb}$ ,  $x=0.01-0.10$ , for different variants of the spatial arrangement of atoms is performed. To model energetic and kinetic performances, particularly the behavior of the Fermi level  $\varepsilon_F$ , the bandgap  $\varepsilon_g$ , the *density of states* (DOS) distribution was calculated for an ordered variant of the structure in which Co atoms at position 4c are replaced by Mn atoms. Substitution of Co atoms ( $3d^74s^2$ ) by Mn ( $3d^54s^2$ ) generates structural defects of acceptor nature in the  $\text{TiCo}_{1-x}\text{Mn}_x\text{Sb}$  semiconductor (the Mn atom contains fewer 3d- electrons than Co). This, at the lowest concentrations of impurity atoms Mn, leads to the movement of the Fermi level  $\varepsilon_F$  from the conduction band  $\varepsilon_C$  to the depth of the bandgap  $\varepsilon_g$ . In a semiconductor with the composition  $\text{TiCo}_{0.99}\text{Mn}_{0.01}\text{Sb}$ , the Fermi level  $\varepsilon_F$  is located in the middle of the bandgap  $\varepsilon_g$ , indicating its maximum compensation when the concentrations of ionized acceptors and donors are close. At higher concentrations of impurity Mn atoms, the number of generated acceptors will exceed the concentration of donors, and the concentration of free holes will exceed the concentration of electrons. Under these conditions, the Fermi level  $\varepsilon_F$  approach, and then the level of the valence band  $\varepsilon_V$   $\text{TiCo}_{1-x}\text{Mn}_x\text{Sb}$  cross: the dielectric-metal conductivity transition take place.

The presence of a high-temperature activation region on the temperature dependence of the resistivity  $\ln(\rho(1/T))$   $\text{TiCo}_{1-x}\text{Mn}_x\text{Sb}$  at the lowest concentration of impurity atoms Mn,  $x=0.01$ , indicates the location of the Fermi level  $\varepsilon_F$  in the bandgap  $\varepsilon_g$  of the semiconductor thermopower coefficient  $\alpha(T,x)$  at these temperatures specify its position - at a distance of  $\sim 6$  meV from the level of the conduction band  $\varepsilon_C$ . In this case, electrons are the main carriers of current. The absence of a low-temperature activation region on this dependence indicates the absence of the jumping mechanism  $\varepsilon_3^p$  conductivity. Negative values of the thermopower coefficient  $\alpha(T,x)$   $\text{TiCo}_{0.99}\text{Mn}_{0.01}\text{Sb}$  at all temperatures, when according to DOS calculations the concentrations of acceptors and donors are close, and the semiconductor is maximally compensated, can be explained by the higher concentration of uncontrolled donors. However, even at higher concentrations of impurity Mn atoms in  $\text{TiCo}_{0.98}\text{Mn}_{0.02}\text{Sb}$ , the sign of the thermopower coefficient  $\alpha(T,x)$  remains negative, but the value of resistivity  $\rho(x, T)$  increases rapidly, and the Fermi level  $\varepsilon_F$  deepens into the forbidden zone at a distance of  $\sim 30$  meV. The rapid increase in the values of the resistivity  $\rho(x, T)$  in the region of concentrations  $x=0.01-0.02$  shows that acceptors are generated in the  $\text{TiCo}_{1-x}\text{Mn}_x\text{Sb}$  semiconductor when Co atoms are replaced by Mn, which capture free electrons, reducing their concentration. However, negative values of the thermopower coefficient  $\alpha(T,x)$  are evidence that either the semiconductor has a significant concentration of donors, which is greater than the number of introduced acceptors ( $x=0.02$ ), or the crystal simultaneously generates defects of acceptor and donor nature. The obtained result does not agree with the calculations of the electronic structure of the  $\text{TiCo}_{1-x}\text{Mn}_x\text{Sb}$  semiconductor. It is concluded that more complex structural changes occur in the semiconductor than the linear substitution of Co atoms by Mn, which simultaneously generate structural defects of acceptor and donor nature by different mechanisms, but the concentration of donors exceeds the concentration of generated acceptors.

Based on a comprehensive study of the electronic structure, kinetic and energetic performances of the thermosensitive material  $\text{TiCo}_{1-x}\text{Mn}_x\text{Sb}$ , it is shown that the introduction of impurity Mn atoms into  $\text{TiCoSb}$  can simultaneously generate an acceptor zone  $\varepsilon_A$  (substitution of Co atoms for Mn) and donor zones  $\varepsilon_D^1$  and  $\varepsilon_D^2$  of different nature. The ratio of the concentrations of ionized acceptors and donors generated in  $\text{TiCo}_{1-x}\text{Mn}_x\text{Sb}$  will determine the position of the Fermi level  $\varepsilon_F$  and the mechanisms of electrical conductivity. However, this issue requires additional research, in particular structural and modeling of the electronic structure of a semiconductor solid solution under different conditions of entry into the structure of impurity Mn atoms. The investigated solid solution  $\text{TiCo}_{1-x}\text{Mn}_x\text{Sb}$  is a promising thermometric material.

**Key words:** Electronic structure, Resistivity, Thermopower.

## 1. Introduction

One of the ways to obtain semiconductor thermometric materials based on semi-Geisler phases is to generate in the crystal structural defects of donor and/or acceptor nature, which changes the value of the thermopower coefficient, resistivity, and thermal conductivity [1]. The study presents the first results of researches about a new thermometric material based on a solid solution obtained by doping a basic TiCoSb semiconductor (Str. Type MgAgAs, eg group  $F\bar{4}3m$ ) with Mn atoms by replacing Co. In [1], the semi-Geisler phase of TiCoSb was studied, as well as thermometric materials based on it:  $TiCo_{1-x}Ni_xSb$ ,  $TiCo_{1-x}Cu_xSb$ ,  $Ti_{1-x}V_xCoSb$ ,  $Ti_{1-x}Mo_xCoSb$ ,  $Ti_{1-x}Sc_xCoSb$ . Consequently, was shown that the structure of the TiCoSb compound is defective: in position 4a of the Ti atoms there are vacancies ( $V_a$ ) (till ~ 1%), and in the tetrahedral voids, which occupy ~ 24% of the unit cell volume, there are additional  $Co^*$  atoms (up to ~ 1%). In this case, the formula of the compound TiCoSb is transformed into  $(Ti_{0.99}Va_{0.01})Co(Co^*_{0.01})Sb$ . In this case, the formula of the compound TiCoSb is transformed into  $(Ti_{0.99}Va_{0.01})Co(Co^*_{0.01})Sb$ . The presence of  $V_a$  vacancies in the position of Ti atoms leads to the generation of structural defects of acceptor nature in the crystal, and the corresponding acceptor levels (zone)  $\varepsilon_A$  appear in the bandgap  $\varepsilon_g$ . In turn, additional  $Co^*$  atoms in tetrahedral cavities generate structural defects of donor nature, and donor levels (zone)  $\varepsilon_D$  appear in the bandgap  $\varepsilon_g$ . This is the mechanism of "a priori doping" of the TiCoSb semiconductor with donor and acceptor impurities.

Because the Fermi level  $\varepsilon_F$  in TiCoSb is located between the energy states of donors and acceptors, the smallest changes in the ratio between them, caused, for example, by the modes of thermal annealing of samples and their cooling, purity of initial components, etc., change the position of Fermi level  $\varepsilon_F$  and zones of continuous energies of the semiconductor. That is why in the temperature range  $T < 90$  K TiCoSb is a semiconductor of the hole type conductivity, which is indicated by positive values of the thermopower coefficient  $\alpha$ , and at higher temperatures the main current carriers are electrons. This change in the type of main current carriers depending on the temperature also indicates a different depth of energy levels: the acceptor levels are small impurities and are located closer to the zone of continuous energies than the donor ones.

The study of semiconductor thermometric materials  $Ti_{1-x}V_xCoSb$  and  $Ti_{1-x}Mo_xCoSb$  showed that the crystal simultaneously generates defects of acceptor nature in the form of vacancies in the positions of Ti and Co atoms, and the occupation of atoms V or Mo position 4a by Ti atoms generates defects of donor nature. The mechanism of simultaneous appearance of

acceptors and donors provides the semiconductor properties of  $Ti_{1-x}V_xCoSb$  and  $Ti_{1-x}Mo_xCoSb$ . Doping of the TiCoSb semiconductor with Sc atoms introduced by substituting Ti atoms generates defects of acceptor nature, and the ratio of defects of donor and acceptor nature in  $Ti_{1-x}Sc_xCoSb$  determines the location of the Fermi level  $\varepsilon_F$  and conduction mechanisms.

The study of the semiconductor solid  $TiCo_{1-x}Ni_xSb$  revealed a linear change in the values of the period of the unit cell  $a(x)$ , which indicates the substitution of only Co atoms for Ni. In this case, donors are generated in the crystal, because the atom Co ( $3d^74s^2$ ) has a smaller number of 3d electrons than the atom Ni ( $3d^84s^2$ ).  $TiCo_{1-x}Cu_xSb$  also has a different reaction of structural parameters depending on the impurity concentration.

The results of the study of energetic and kinetic performances of semiconductor thermometric material  $TiCo_{1-x}Mn_xSb$ ,  $x=0.01-0.10$ , as well as their comparison with the results of modeling the electronic structure will identify the mechanisms of electrical conductivity to determine the synthesis of thermosensitive materials with maximum efficiency of thermal energy conversion.

## 2. Limitations

Studies of thermometric materials based on TiCoSb [1] have established their high sensitivity to heat treatment modes (temperature and duration of annealing).

## 3. Research objective

To establish the nature of structural defects in the thermometric material  $TiCo_{1-x}Mn_xSb$ , which will identify the mechanisms of electrical conductivity and determine the conditions of their synthesis to obtain maximum efficiency of conversion of thermal energy into electricity.

## 4. Research methods

Samples of  $TiCo_{1-x}Mn_xSb$  were synthesized by fusing the charge of the source components in an electric arc furnace in an inert atmosphere followed by homogenizing annealing for 720 h at a temperature of 1073 K. by the method of X-ray diffraction analysis (powder method) obtained data sets (diffractometer DRON-4.0,  $FeK\alpha$ -radiation), and with the help of the program, Fullprof [2] the structural characteristics of  $TiCo_{1-x}Mn_xSb$  were calculated. The chemical and phase compositions of the samples were monitored by metallographic analysis (scanning electron microscope REMMA-102-02).

Modeling of the electronic structure of  $TiCo_{1-x}Mn_xSb$  was performed by the KKR (Coring-Kon-Rostocker method) in the approximation of coherent

potential (Coherent Potential Approximation, CPA) and local density (Local Density Approximation, LDA) [3]. The calculations used licensed software AkaiKKR and SPR-KKR in the LDA approximation for the exchange-correlation potential with parameterization Moruzzi-Janak-Williams (MJW) [4]. To model the energy characteristics of  $\text{TiCo}_{1-x}\text{Mn}_x\text{Sb}$ , the density distribution of electronic states (DOS) was calculated, and the Brillouin zone was divided into 1000  $k$ -points. The width of the energy window was 22 eV and was chosen to capture all semi-core states of p-elements. The accuracy of calculating the position of the Fermi level  $\varepsilon_F \pm 4$  meV.

Temperature and concentration dependences of resistivity ( $\rho$ ) and the thermopower coefficient ( $\alpha$ ) relative to copper  $\text{TiCo}_{1-x}\text{Mn}_x\text{Sb}$  were measured in the ranges:  $T = 80\text{--}400$  K,  $x = 0.01\text{--}0.10$ .

## 5. Research of structural characteristics $\text{TiCo}_{1-x}\text{Mn}_x\text{Sb}$

Microprobe analysis of the concentration of atoms on the surface of  $\text{TiCo}_{1-x}\text{Mn}_x\text{Sb}$  samples, including the composition  $x = 0\text{--}0.10$ , established their correspondence to the initial compositions of the charge (Fig. 1)

In turn, X-ray phase analysis showed no traces of extraneous phases on the diffractograms of the studied  $\text{TiCo}_{1-x}\text{Mn}_x\text{Sb}$  samples except for the main phase (Fig. 2), which is indexed in the structural type of MgAgAs. The obtained results testify to the homogeneity of the samples and their suitability for the study of electrokinetic characteristics and the manufacture of sensitive elements of thermoelectric sensors.

Therefore, the structural studies of the semiconductor thermometric material  $\text{TiCo}_{1-x}\text{Mn}_x\text{Sb}$  allow speaking about the ordering of its crystal structure, and the substitution of Co atoms at Mn at position 4c will generate structural defects of acceptor nature.

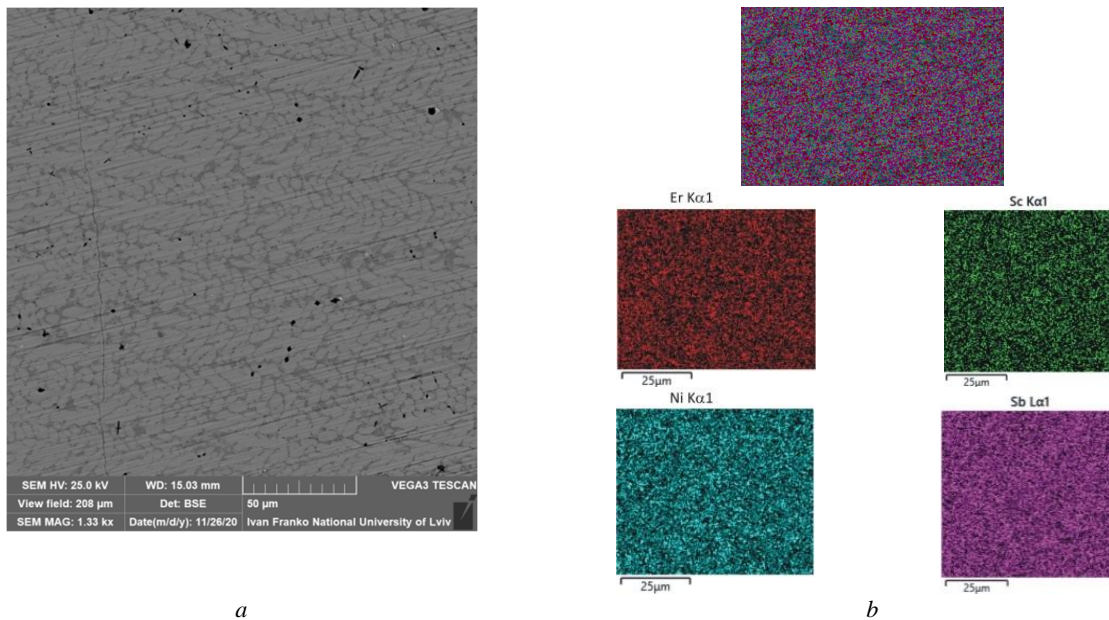


Fig. 1. Photograph of the surface (a) and distribution of elements (b) in the sample  $\text{TiCo}_{0.95}\text{Mn}_{0.05}\text{Sb}$

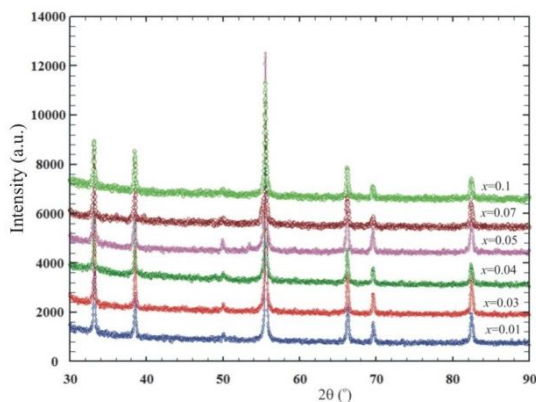


Fig. 2. Diffractograms of samples of thermometric material  $\text{TiCo}_{1-x}\text{Mn}_x\text{Sb}$

## 6. Modeling of the electronic structure of thermometric material $\text{TiCo}_{1-x}\text{Mn}_x\text{Sb}$

To model the energetic and kinetic characteristics of the semiconductor thermometric material  $\text{TiCo}_{1-x}\text{Mn}_x\text{Sb}$ , in particular, the behavior of the Fermi level  $\varepsilon_F$ , bandgap width  $\varepsilon_g$ , the density of states (DOS) was calculated (Fig. 3) for an ordered variant of the structure, in which Co atoms in position 4c are replaced by Mn atoms. As can be seen from Fig. 3, in the semi-Geisler phase of  $\text{TiCoSb}$ , the Fermi level  $\varepsilon_F$  (dashed line) is located in the bandgap  $\varepsilon_g$  near its middle, but closer to the edge of the conduction band  $\varepsilon_C$ , which is characteristic of semiconductors of electronic conduc-



tivity type. Because the substitution of Co atoms ( $3d^74s^2$ ) by Mn ( $3d^54s^2$ ) generates structural defects of acceptor nature in the semiconductor (the Mn atom contains fewer  $3d$  electrons than Co), then even at the lowest concentrations of impurity atoms Mn the Fermi level  $\varepsilon_F$  begins to drift from the conduction band  $\varepsilon_C$  to the depth of the bandgap  $\varepsilon_g$ .

In a semiconductor with the composition  $\text{TiCo}_{0.99}\text{Mn}_{0.01}\text{Sb}$ , the Fermi level  $\varepsilon_F$  is located in the middle of the bandgap  $\varepsilon_g$ , indicating its maximum compensation when the concentrations of ionized acceptors and donors are close. In the experiment, the approximation of the Fermi level  $\varepsilon_F$  to the middle of the bandgap  $\varepsilon_g$  should be accompanied by a sharp increase in the resistivity values  $\rho(x, T)$ , as free electrons and holes are captured by acceptors and donors.

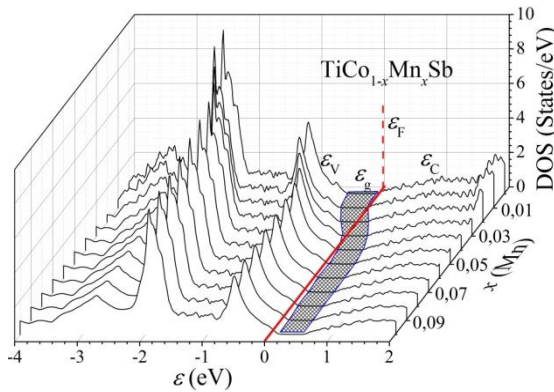


Fig. 3. The density of electronic states of  $\text{TiCo}_{1-x}\text{Mn}_x\text{Sb}$  for an ordered variant of the structure

At higher concentrations of Mn, the number of generated acceptors exceeds the concentration of donors, and the concentration of free holes exceeds the concentration of electrons. Under these conditions, the Fermi level  $\varepsilon_F$  approaches, and then the level of the valence band  $\varepsilon_V$   $\text{TiCo}_{1-x}\text{Mn}_x\text{Sb}$  crosses: the dielectric-metal conductivity transition takes place. The experiment should change the sign of the thermopower coefficient  $\alpha(x, T)$   $\text{TiCo}_{1-x}\text{Mn}_x\text{Sb}$  from negative to positive, and the intersection of the Fermi level  $\varepsilon_F$  and the valence band  $\varepsilon_V$  changes the conductivity from activation to metallic: on the dependences  $\ln(\rho(1/T))$  the activation sites disappear, and the values of resistivity  $\rho$  increase with temperature. The results of kinetic and energetic studies of  $\text{TiCo}_{1-x}\text{Mn}_x\text{Sb}$  show the correspondence of these calculations to real processes in a semiconductor.

## 7. Research of electrokinetic and energetic characteristics of thermometric material $\text{TiCo}_{1-x}\text{Mn}_x\text{Sb}$

*A priori* predicted that the kinetic characteristics of  $\text{TiCo}_{1-x}\text{Mn}_x\text{Sb}$  samples appear features caused in the first place: the electronic configuration of the Mn atom

( $3d^54s^2$ ) which may change as the  $4s$  electron transitions to the  $3d$  shell and forms a  $3d^64s^1$  configuration with a single valence collectivized  $4s$  electron. The second feature of the Mn atom is the presence of a local magnetic moment caused by the presence of unpaired  $3d$ -electrons due to the idleness of their  $3d$ -shell, which will affect the mechanisms of electric current scattering.

Temperature and concentration dependences of specific electrical resistance  $\rho$  and the thermopower coefficient  $\alpha$   $\text{TiCo}_{1-x}\text{Mn}_x\text{Sb}$  are shown in Fig. 4-5. As can be seen from Fig. 4, for samples  $\text{TiCo}_{1-x}\text{Mn}_x\text{Sb}$  dependences  $\ln(\rho(1/T))$  are characteristic of semiconductors and are approximated by the known relation [5] (1):

$$\rho^{-1}(T) = \rho_1^{-1} \exp\left\{-\frac{\varepsilon_1^r}{k_B T}\right\} + \rho_3^{-1} \exp\left\{-\frac{\varepsilon_3^r}{k_B T}\right\} \quad (1)$$

where the first high-temperature term describes the activation of current carriers  $\varepsilon_1^r$  from the Fermi level  $\varepsilon_F$  to the level of continuous energy zones, and the second, low-temperature term, the hopping conductivity at impurity donor states  $\varepsilon_3^r$  with energies close to the Fermi level  $\varepsilon_F$ . The exception is the behavior of the resistivity  $\rho$  for the sample composition  $\text{TiCo}_{1-x}\text{Mn}_x\text{Sb}$ ,  $x=0.05$  when the resistance values  $\rho$  increase with increasing temperature, which is a sign of the metallic type of conductivity (metallic conductivity).

In turn, the temperature dependences of the thermopower coefficient  $\alpha(1/T)$   $\text{TiCo}_{1-x}\text{Mn}_x\text{Sb}$  (Fig. 3) are described by the known expression (2):

$$\alpha = \frac{k_B}{e} \frac{\varepsilon_i^a}{k_B T} - g + 1 \quad (2)$$

where  $\gamma$  is a parameter that depends on the nature of the scattering mechanism. From the high-temperature region of the  $\alpha(1/T)$  dependence, the values of the activation energy  $\varepsilon_i^a$  are calculated, which, as shown in [1], are proportional to the amplitude of large-scale fluctuations of the continuous energy zones of the high-alloy and compensated semiconductor.

The fact that in the sample at the lowest concentration of impurity atoms Mn,  $x=0.01$ , on the temperature dependence of the resistivity  $\ln(\rho(1/T))$  there is a high-temperature activation region (Fig. 4) indicates the location of the Fermi level  $\varepsilon_F$  in the bandgap  $\varepsilon_g$  of the semiconductor, and the negative values of the thermopower coefficient  $\alpha(T, x)$  at these temperatures specify its position - at a distance of  $\sim 6$  meV from the level of the conduction band  $\varepsilon_C$  (Figs. 4, 5). In this case, electrons are the main carriers of current. The absence of a low-temperature activation region on this dependence indicates the absence of the jumping mechanism  $\varepsilon_3^r$  conductivity.

It is known that the activation energy of the jumping conductivity  $\varepsilon_3^r$  shows the degree of electron filling of small-scale fluctuations [5]. As soon as the electrons fill the small-scale fluctuations, the activation

of electrons between potential wells is absent: the dependence of the resistivity  $\ln(\rho(1/T))$  is absent low-temperature activation region. It is obvious that in  $\text{TiCo}_{0.99}\text{Mn}_{0.01}\text{Sb}$  at all investigated temperatures there is a significant number of donors, which exceeds the concentration of introduced acceptors, which leads to overlapping of wave functions of electrons of impurity states near the Fermi level  $\varepsilon_F$  and, as a consequence, of the absence of a jumping mechanism  $\varepsilon_3^0$  (Fig. 4).

Negative values of the thermopower coefficient  $\alpha(T,x)$   $\text{TiCo}_{0.99}\text{Mn}_{0.01}\text{Sb}$  at all temperatures (Fig. 4, 5), when according to DOS calculations (Fig. 3) the concentrations of acceptors and donors are close, and the semiconductor is maximum compensated, can be explained by a slightly higher concentration of uncontrolled donors over acceptors. However, even with a higher concentration of impurity Mn atoms in  $\text{TiCo}_{0.98}\text{Mn}_{0.02}\text{Sb}$ , the sign of the thermopower coefficient  $\alpha(T,x)$  remains negative, but the value of the resistivity  $\rho(x, T)$ , increases rapidly, for example, at a

temperature  $T = 80 \text{ K}$  from  $\rho(x=0.01) \approx 341 \mu\Omega \cdot \text{m}$  to  $\rho(x=0.02) \approx 2612 \mu\Omega \cdot \text{m}$  (Fig. 4). The sample becomes more compensated, and a low-temperature activation region appears on the  $\ln(\rho(1/T))$  dependence, indicating the presence of a jumping mechanism  $\varepsilon_3^0$  conductivity. This is also indicated by the change in the position of the Fermi level  $\varepsilon_F$  in the sample  $\text{TiCo}_{0.98}\text{Mn}_{0.02}\text{Sb}$ , which went deep into the bandgap at a distance of  $\sim 30 \text{ meV}$  (Fig. 6).

The rapid increase in the values of the resistivity  $\rho(x, T)$  in the region of concentrations  $x=0.01-0.02$  shows that acceptors are generated in the  $\text{TiCo}_{1-x}\text{Mn}_x\text{Sb}$  semiconductor when Co atoms are replaced by Mn, which capture free electrons, reducing their concentration. However, negative values of the thermopower coefficient  $\alpha(x, T)$  are evidence that either the semiconductor has a significant concentration of donors, which is greater than the number of introduced acceptors ( $x=0.02$ ), or the crystal simultaneously generates defects of acceptor and donor nature.

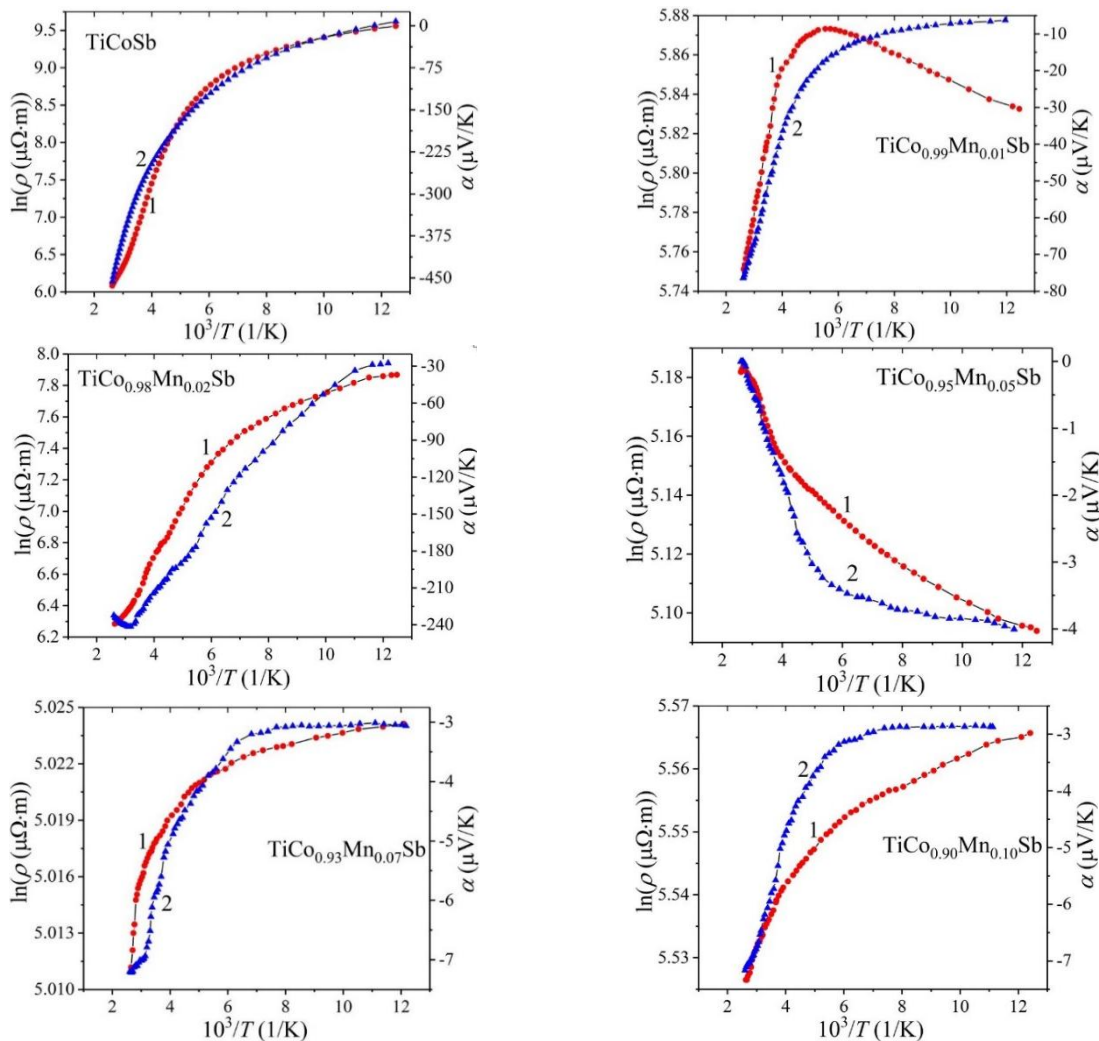


Fig. 4. Temperature dependences of specific electrical resistance  $\ln(\rho(1/T))$  (1) and the thermopower coefficient  $\alpha(1/T)$  (2)  $\text{TiCo}_{1-x}\text{Mn}_x\text{Sb}$

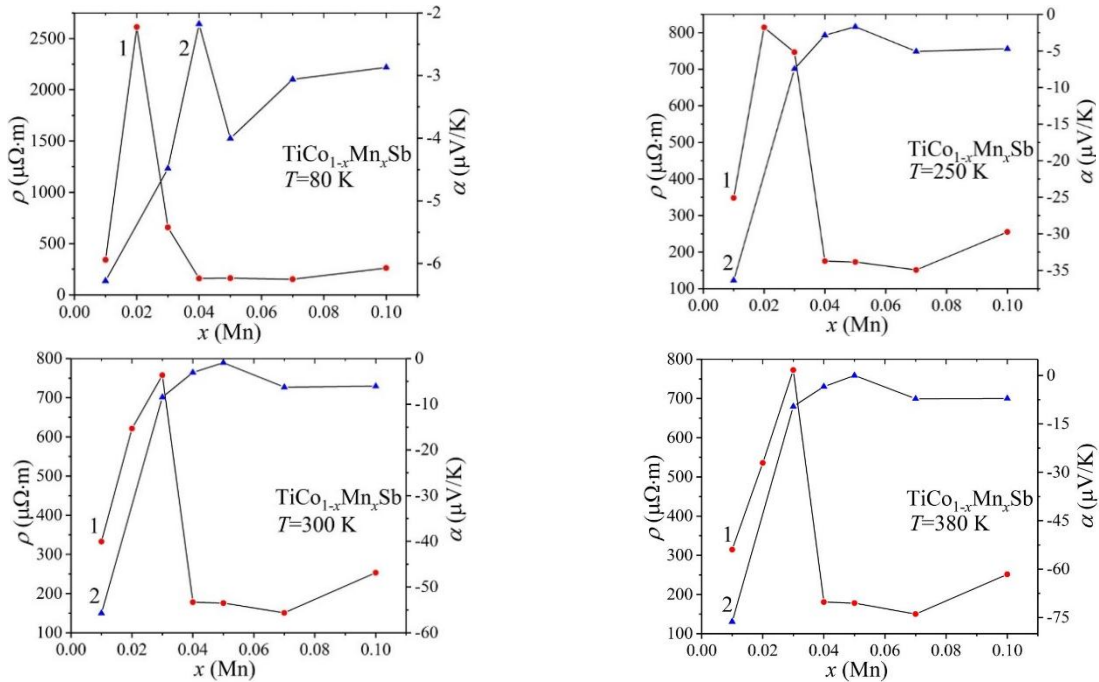


Fig. 5. Change in the values of resistivity  $\rho(x, T)$  (1) and the coefficient of the thermopower coefficient  $\alpha(x, T)$  (2)  $TiCo_{1-x}Mn_xSb$  at different temperatures

The maximum on the dependence of  $\rho(x, T)$   $TiCo_{1-x}Mn_xSb$  at any temperature (Fig. 5) shows that the concentrations of ionized acceptors and donors presented in the semiconductor are balanced, but the number of places at the acceptor levels is slightly less than the number of free electrons.

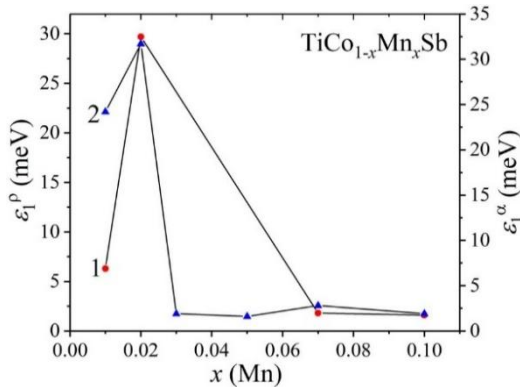


Fig. 6. Change of values of activation energies  $\epsilon_1^p$  (1) and  $\epsilon_1^a$  (2)  $TiCo_{1-x}Mn_xSb$

At a temperature of 80 K, it is necessary to introduce an impurity Mn  $x=0,02$ , which generates acceptors, so that the concentrations of holes and electrons were close. At higher temperatures, deep donor states are ionized, which increases the electron concentration, and therefore the maximum on the dependence  $\rho(x, T)$  appears at higher concentrations of Mn (maximum  $\rho(x, T)$  with temperature shifts to the right). Such a shift of the maximum on the dependence of  $\rho(x, T)$   $TiCo_{1-x}Mn_xSb$  with increasing temperature may indicate the existence of

several mechanisms of formation in the semiconductor of donor levels (zones) of different nature, which are energetically separated in the bandgap  $\epsilon_g$ .

The obtained result does not agree with the calculations of the electronic structure of the semiconductor  $TiCo_{1-x}Mn_xSb$  (Fig. 3). After all, if  $TiCo_{1-x}Mn_xSb$  replaces Co atoms ( $3d^74s^2$ ) with Mn atoms ( $3d^54s^2$ ), acceptors must be generated in the crystal, which captures all free electrons at the concentration of Mn atoms,  $x \approx 0.02$ . The thermopower coefficient sign  $\alpha$  must have positive values and the holes are the main current carriers. Can be assumed that more complex structural changes occur in the semiconductor than the linear replacement of Co atoms by Mn, which simultaneously generate structural defects of acceptor and donor nature by different mechanisms, but the concentration of donors exceeds the concentration of generated acceptors.

Unexpected is the behavior of the kinetic characteristics of  $TiCo_{1-x}Mn_xSb$  at a concentration of  $x=0.05$ . The activation regions disappear on the  $\ln(\rho(1/T))$  dependence, indicating the metallic nature of the electrical conductivity, and the negative values of the thermopower coefficient  $\alpha(T, x)$  indicate the intersection of the Fermi levels  $\epsilon_F$  and the conduction band  $\epsilon_C$ . By introducing a giant concentration of acceptor impurity into the sample, we were unable to change the conductivity type of  $TiCo_{1-x}Mn_xSb$ . The opposite reaction occurred - the concentration of free electrons of unknown nature increased.

At higher concentrations of impurity Mn atoms ( $x \geq 0.07$ ) on the temperature dependences of the

resistivity  $\ln(\rho(1/T))$   $\text{TiCo}_{1-x}\text{Mn}_x\text{Sb}$  appear high- and low-temperature activation sites, from which the activation energies of electrons from the Fermi level  $\varepsilon_F$  to the level of the conduction, band flow are calculated since the sign of the thermopower coefficient  $\alpha(T,x)$  remains negative:  $\varepsilon_1^p$  ( $x=0.07$ )=1.8 meV and  $\varepsilon_1^p$  ( $x=0.10$ )=1.6 meV (Fig. 6). This course  $\ln(\rho(1/T))$   $\text{TiCo}_{1-x}\text{Mn}_x\text{Sb}$  dependences is possible only under the condition of semiconductor compensation (simultaneous existence of ionized donors and acceptors). In turn, low values of activation energies  $\varepsilon_1^p$  indicate the location of the Fermi level  $\varepsilon_F$  near the level of the conduction band, which is possible under the condition of weak compensation of the semiconductor, when the concentration of free electrons is much higher than the hole concentration.

What is the reason for such, at first glance, illogical behavior of kinetic and energetic characteristics in the  $\text{TiCo}_{1-x}\text{Mn}_x\text{Sb}$  semiconductor?

Recall that the authors of [1] found that in the structure of the basic compound  $\text{TiCoSb}$  simultaneously exist ~ 1% vacancy ( $V_a$ ) in position  $4a$  of Ti atoms, which generates structural defects of acceptor nature, and in the bandgap  $\varepsilon_g$  there is a corresponding acceptor level (zone)  $\varepsilon_A$ . Also, the tetrahedral voids of the  $\text{TiCoSb}$  structure contain ~ 1% of additional  $\text{Co}^*$  atoms, which generates structural defects of donor nature, and the corresponding donor level (zone)  $\varepsilon_D^1$  will appear in the bandgap  $\varepsilon_g$ . Ordering the structure of  $\text{TiCo}_{1-x}\text{Mn}_x\text{Sb}$  and the absence of vacancies in position  $4a$  generates a donor zone  $\varepsilon_D^1$ . Another mechanism for generating donor states (zones  $\varepsilon_D^2$ ) is the partial occupation of tetrahedral voids of the structure by impurity Mn atoms.

Therefore, the introduction of impurity Mn atoms into  $\text{TiCoSb}$  can simultaneously generate in the semiconductor the acceptor zone  $\varepsilon_A$  (substitution of Co atoms for Mn) and the donor zones  $\varepsilon_D^1$  and  $\varepsilon_D^2$  of different nature. The ratio of the concentrations of ionized acceptors and donors generated in  $\text{TiCo}_{1-x}\text{Mn}_x\text{Sb}$  determines the position of the Fermi level  $\varepsilon_F$  and the mechanisms of electrical conductivity. However, this issue requires additional research, in particular structural

and modeling of the electronic structure of a semiconductor solid solution under different conditions of entry into the structure of impurity Mn atoms.

## 8. Conclusions

Based on a comprehensive study of the electronic structure, kinetic and energetic characteristics of the thermosensitive material  $\text{TiCo}_{1-x}\text{Mn}_x\text{Sb}$ , it is established that to ensure the *stability* of the structure and the principle of electroneutrality in the *semiconductor* simultaneously generated structural defects of acceptor and donor nature, the concentration of which grows with increasing content of Mn atoms. The investigated solid solution  $\text{TiCo}_{1-x}\text{Mn}_x\text{Sb}$  is a promising thermometric material.

## 9. Gratitude

The authors are grateful to the members of the scientific seminar of the Department of Information-Measuring Technologies of Lviv Polytechnic National University for an interesting and informative discussion on the results of these researches.

## 10. Conflict of interests

The authors declare that there is no financial or other possible conflict related to this work.

## References

- [1] V. Romaka, Yu. V. Stadnyk, V. Krayovskyy, L. Romaka, O. Huk, V. Romaka, M. Mykyichuk, A. Horyn, *The modern heat-sensitive materials and temperature transducers*. Lvivska Polytechnika, 2020.
- [2] T. Roisnel, J. Rodriguez-Carvajal, "WinPLOTR: a Windows Tool for Powder Diffraction Patterns analysis", *Materials Science Forum*, vol. 378–381, pp. 118–123, 2001.
- [3] M. Schruter, H. Ebert, H. Akai, P. Entel, E. Hoffmann, G. Reddy, "First-principles investigations of atomic disorder effects on magnetic and structural instabilities in transition-metal alloys", *Physical Review. B*, vol. 52, pp. 188–209, 1995.
- [4] V. Moruzzi, J. Janak, A. Williams, *Calculated Electronic Properties of Metals*. NY, Pergamon Press, 1978.
- [5] B. Shklovskii, A. Efros, *Electronic Properties of Doped Semiconductors*. NY, Springer, 1984.